Environmental Earth Sciences (2019) 78:258
https://doi.org/10.1007/s12665-019-8261-9

ORIGINAL ARTICLE

Exploring the potential for groundwater inundation in coastal US cities due to interactions between sewer infrastructure and global change

Robert J. Rossi[1,2] · Laura Toran[1]

Received: 11 January 2019 / Accepted: 4 April 2019

Abstract
Urbanization, in particular, the culverting and burying of streams in sewer infrastructure, has affected both surface and subsurface flow regimes. While researchers have examined the impact of stream burial on groundwater budgets, field studies examining the influence of urbanization on groundwater dynamics are relatively scarce. This study analyzes tidal patterns in water-level data from shallow groundwater monitoring wells located next to a legacy sewer line within the city of Philadelphia, Pennsylvania, USA. The coupling of historic records, sewer network maps, and well bore hydrogeology explains spatial patterns in groundwater elevations. Furthermore, a synthesis of early twentieth century United States census data, and continental scale GIS data demonstrates the potential for groundwater inundation in coastal United States cities that are served by aging sewer infrastructure. Altered groundwater flow dynamics caused by sea level rise, coupled with climatic shifts will likely stress aging sewer infrastructure, and can lead to increased discharge of combined sewer overflow systems and flooding.

Keywords Urban groundwater · Heterogeneity · Sewers · Climate change · Coastal aquifers

Introduction

Between 1970 and 2000, global urban land area has increased by over 50,000 km^2 (Seto et al. 2011), and by 2050 the United Nations predicts that 66% of the Earth's population will reside in urban areas (United Nations 2014). Unsurprisingly, urbanization processes have significantly impacted ecosystems and hydrologic cycles. Specifically, a common urbanization practice in the mid to late nineteenth century was to culvert and bury streams in sewer infrastructure (Broadhead et al. 2013, 2015; Hopkins et al. 2013), which can lead to increased loadings of sewage-borne contaminants (e.g., nitrogen-metabolizing species) (Divers et al. 2013), or increase the likelihood of flooding as flow becomes concentrated in the buried channels. In addition to alterations in the surface hydrologic regimes, subsurface hydrologic regimes are also affected by water inflows and outflows to sewer systems.

Consequently, the influence of urban sewer and water conveyance infrastructure on subsurface hydrologic regimes has become an active research area (e.g., Lerner 1986; Ellis et al. 2004; Hibbs and Sharp 2012). Most of the existing literature characterizing impacts of sewer infrastructure on urban groundwater system focuses on the role of exfiltration and infiltration of water from sewage infrastructure in urban water budgets (e.g., Kim et al. 2001; Bhaskar and Welty 2012). However, while the impact of stream burial on subsurface flow budgets is recognized (Sharp 2010), field studies examining the influence of urbanization on groundwater dynamics are relatively scarce. Moreover, the impacts of historic sewage infrastructure on groundwater dynamics in the context of altered hydrologic regimes caused by changes in global climate are not well-characterized.

Electronic supplementary material The online version of this article (https://doi.org/10.1007/s12665-019-8261-9) contains supplementary material, which is available to authorized users.

✉ Robert J. Rossi
robrossi@stanford.edu

[1] Department of Earth and Environmental Science, Temple University, 1901N, 13th Street, Philadelphia, PA 19122, USA

[2] Department of Earth System Science, Stanford University, 473 Via Ortega, Stanford, CA 94305, USA

Published online: 11 April 2019

This study highlights the impact of the subsurface heterogeneity resulting from legacy urbanization activities (e.g., the sewering and burying of streams) on patterns in groundwater dynamics. In particular, this study analyzes tidal patterns in water-level data from shallow groundwater monitoring wells located next to a legacy sewer line within the city of Philadelphia, Pennsylvania, USA. Furthermore, 1907 United States census data and continental scale GIS data are synthesized to demonstrate the potential for unexpected patterns of groundwater inundation in coastal United States cities that are served by aging sewer infrastructure.

Methods

Study area

This study takes place within the city of Philadelphia, the fifth most populous city (2010 population 1,526,006) in the United States (United States Census Bureau Population Division 2017). Philadelphia covers an area of 347 km^2 (United States Bureau of the Census 2010), 48% (165 km^2) of which is served by a combined sewer system (Philadelphia Water Department 2017) (Fig. 1). The city is located in the Schuylkill River and Delaware River watersheds, lies within the Piedmont and Atlantic Coastal Plain physiographic provinces (Pennsylvania Bureau of Topographic and Geologic Survey Department of Conservation and Natural Resources 1995), and surficial geology in the study area consists of Tertiary and Quaternary coastal plain sediments (Berg et al. 1980) along with fill material.

The study site is along the US I-95 corridor, where a series of stormwater control measures (i.e., bioretention basins) are being constructed to improve infiltration next to the roadway expansion. Monitoring wells were installed to provide information on baseline groundwater conditions near the stormwater control measures. All monitoring wells tap an unconfined aquifer contained within the Pleistocene age Trenton gravel (Fig. 1) (Berg et al. 1980; Paulachok 1991). All wells are located approximately 50 km upstream of the saltwater interface on the Delaware

River (Delaware River Basin Commission 2019), and 16 km downstream of the drinking water intake for the city of Philadelphia (Philadelphia Water Department 2014). As such, it is highly unlikely that seawater intrusion occurs within the study area.

Monitoring wells

Seven monitoring wells were installed in March and July 2016 along a southwest–northeast transect paralleling an interstate (US I-95) (Fig. 1). Within the general southwest–northeast transect, a smaller transect of three wells was installed perpendicular to US I-95 to monitor the variation in groundwater level response as a function of distance from the Delaware River (MW1, MW2, and MW3). Of the seven monitoring wells, six wells (MW1, MW2, MW3, MW4, MW5, and MW7) were examined in this study. MW6 was determined to tap a perched water table created by the buried portions of the Dyottville glass works (Bromley and Bromley 1895, 1910), and was not considered in further analysis.

Wells were cased with 5.08 cm polyvinyl chloride (PVC) and drilled to 8.7–9.7 m with a 1.5 m screen at the bottom. A well boring report was completed by Susquehanna Civil Inc. for each well. Each boring report records both sedimentological (e.g., Unified Soil Classification System soil texture) and hydrological (e.g., relative moisture content) properties (electronic supplementary material, Table S1).

Data from water level loggers were used to record storm events, tidal conditions, and water levels between storm events. Onset Hobo water level loggers (U20L-001-04) were installed in the monitoring wells in April 2016. Onset Hobo loggers have an operational range of 0–4 m water depth, measure changes in water levels with a resolution of 0.14 cm, and measure water levels with an accuracy of 0.4 cm.

Hydraulic conductivity calculations

The hydrologic conductivities of aquifer sediments in monitoring wells were measured between May and June 2017 well using the Hvorslev slug test analysis method (Fetter 2001). In particular, the basic Hvorslev equation was used as the screened length of the studied monitoring wells is greater than eight times the radius of the well screen:

$$K = \frac{r^2 \times \ln\left(L/r_w\right)}{2 \times L \times t_{37}}, \tag{1}$$

where r is the radius of the well casing (m), L is the length of the well screen (m), r_w is the radius of the well screen (m), and t_{37} is the time when the water level rises or falls to 37% of the initial hydraulic head H_0 (m). The slug used consisted of a 4 cm by 55 cm long PVC schedule 40 pipe filled with sand. During the slug test, water levels were logged with an Onset Hobo U20L-001-04 logger set to 10 s logging intervals.

Hydraulic conductivities of aquifer sediments were also determined using the Jacob–Ferris tidal methods (Jacob 1950; Ferris 1951). First the true tidal efficiency was calculated:

$$\mathrm{TE}_{\mathrm{true}} = \frac{\alpha}{\alpha + \theta\beta}, \tag{2}$$

where α is the compressibility of the aquifer skeleton (in Pa^{-1}), θ is the aquifer porosity, and β is the compressibility of H_2O at 15 °C (46.7×10^{-11} Pa^{-1}). Estimates of aquifer

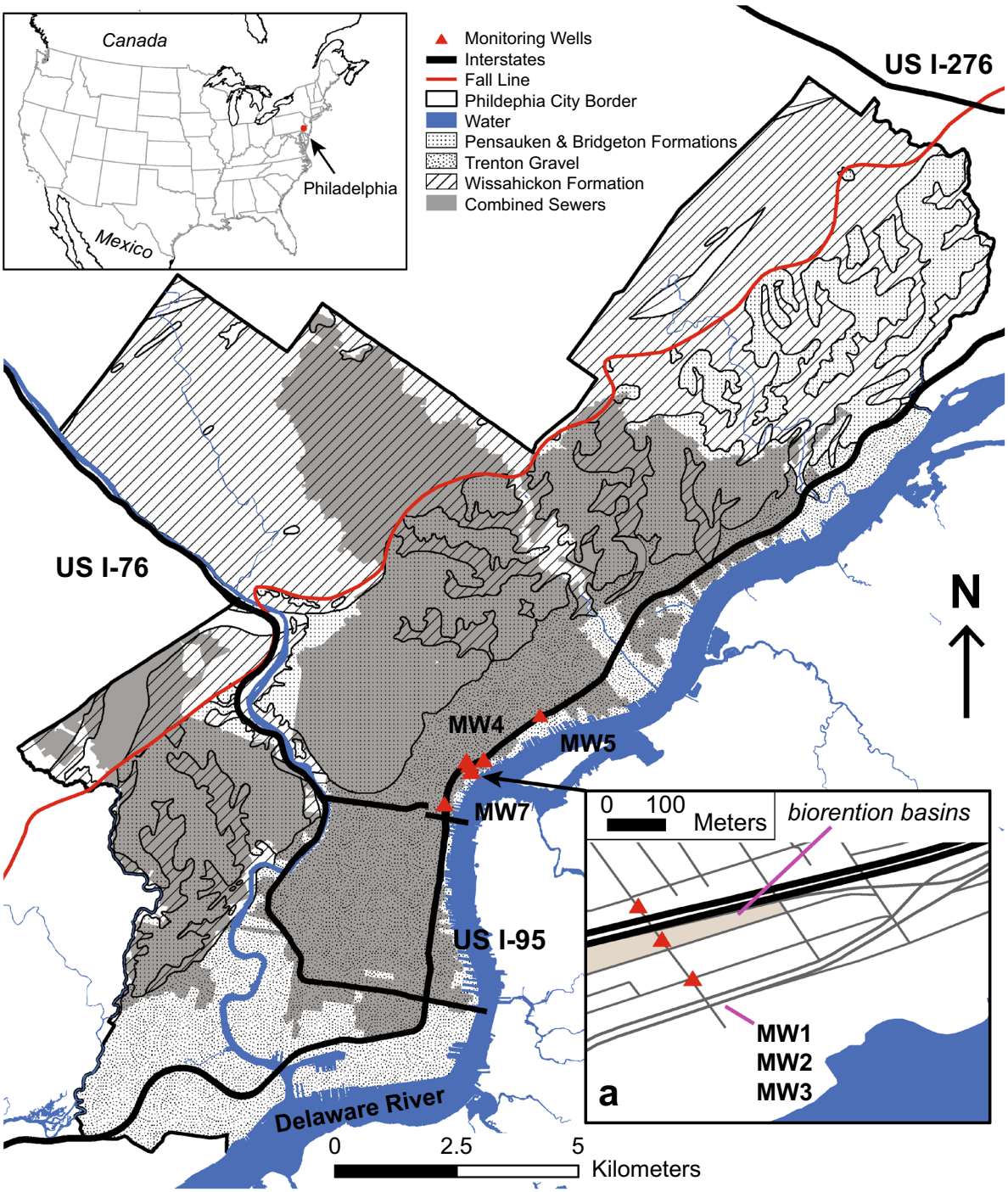

Fig. 1 Map of the city of Philadelphia showing the locations of the sampled monitoring wells, major interstates (Pennsylvania Department of Transportation Bureau of Planning and Research Geographic Information Division 2017), surficial geology (Miles et al. 2001), the area serviced by a combined sewer system (Philadelphia Water Department 2017) the approximate location of the Atlantic Fall Line (Pennsylvania Bureau of Topographic and Geologic Survey Department of Conservation and Natural Resources 1995), and an inset (a) detailing the monitoring well transect (triangles), their orientation relative to US I-95 (black line), local roads (grey lines), and nearby bioretention basins (shaded area)

properties used in the tidal efficiency calculations are provided in the electronic supplementary material (Table S2).

Next, the results of (2) were used to calculate the specific storage of the aquifer (S_s):

$$S_s = \frac{\theta\beta\gamma}{1 - \mathrm{TE}_{\mathrm{true}}}, \tag{3}$$

where θ is the previously estimated aquifer porosity, β is the compressibility of H_2O at 15 °C (46.7×10^{-11} Pa^{-1}), and γ is the specific weight of H_2O (9.80×10^{3} Pa m^{-1}).

Finally, the results of (3) were used to calculate the hydraulic conductivity of the aquifer (K in m s^{-1}):

$$K = \frac{S_s t_o x^2}{4\pi \mathrm{Lag}^2}\frac{1}{60}, \tag{4}$$

where S_s is the calculated specific storage, t_o is the period of the tidal oscillation (in min), x is the perpendicular distance inland from the Delaware River shoreline (in m, as determined using the near function in ArcGIS), and Lag is the lag time between well water level fluctuations and tidal fluctuations (in min). Delaware River tidal data were taken from the Philadelphia, PA National Oceanic Atmospheric Association CO-OPs station (ID #8545240), located 4 km south of wells MW1, MW2, and MW3 (NOAA Center for Operational Oceanographic Products and Services 2017). Lag times between groundwater level fluctuations and tidal fluctuations were calculated using the cross-correlation function in R. The period of water level fluctuations was determined using the spectrum function, and fast-Fourier transforms were performed with the fft function in R.

Spatial and statistical analyses

All spatial analyses were conducted in ArcGIS 10.4. The coverage of the main sewerage system in the vicinity of the study area was digitized from a map included in the 1902 annual report of the city of Philadelphia (Philadelphia Department of Public Works Bureau of Surveys 1902). Statistical data of early 20th century United States sewer infrastructure were collected from a 1907 United States Census Bureau special report (United States Bureau of the Census 1907). The proportion of these cities in areas affected by tidal fluctuations was determined by comparing the distance between the extent of the city area (United States Census Bureau 2016) and coastal or estuarine boundaries. Tidally affected reaches of rivers were determined by either examining United States Geological Survey National Water Information System stream gauge records (United States Geological Survey 2017), or reports pertaining to the river of interest. Details of referenced materials for this analysis are provided in Table S2 of the electronic supplementary material (ESM).

Statistical analyses were conducted in the R software (R Core Team 2016).

Results

Water level records

During the period of record the highest observed groundwater levels occur in well MW4 (Table 1). The average water levels recorded in each monitoring suggest that the water table is relatively higher near MW4, creating a mound that extends over to MW1, MW2, and MW3 (Table 1). Within the transect of monitoring wells (MW1, MW2, and MW3) that runs perpendicular to US I-95, water levels are generally the highest in MW2 and lowest in MW1 (Fig. 3, Table 1). This pattern is contrary to the expected slope of the local water table, which should generally decrease moving towards the Delaware River (Paulachok 1991). The cause of this pattern is currently unknown but could represent heterogeneities in aquifer materials. Although groundwater mounding due to the nearby stormwater bioretention basin could be a factor (Machusick et al. 2011), there is not an

Table 1 Seasonal and annual mean groundwater elevations (in meters above sea level) in each well during the period of record (April 2016–May 2017), measured and calculated hydraulic conductivity (K, in m s^{-1}) of each well, and the distance of each well from the shoreline and the nearest sewer main (in meters)

Well	Ave. water level				Annual mean water level	Slug test K	Tidally calculated K	Distance to shore	Distance to sewer main
	Spring	Summer	Fall	Winter					
MW1	1.41	1.52	1.62	1.57	1.54	1.69×10^{-3}	1.67×10^{-3}	480	7.30
MW2	1.65	1.70	1.63	1.62	1.65	2.00×10^{-3}	2.05×10^{-3}	392	7.30
MW3	1.54	1.63	1.58	1.55	1.58	1.65×10^{-3}	1.65×10^{-3}	304	7.30
MW4	2.16	2.17	2.17	2.20	2.18	8.83×10^{-5}	3.23×10^{-5}	210	57.8
MW5	1.14	1.09	0.96	0.96	1.03	9.29×10^{-5}		270	197
MW7	0.65	0.66	0.56	0.52	0.59	1.76×10^{-3}		179	489

observed seasonality to the mounding (e.g., mounding is not higher during wetter seasons).

Hydraulic conductivity results

Slug testing determined that the hydraulic conductivities in the monitoring wells ranged from 4.04×10^{-5} to 2.00×10^{-3} m s^{-1} (Table 1). Hydraulic conductivities are higher in wells MW1, MW2, MW3, and MW7, with the highest hydraulic conductivity observed in MW2. In general, the hydraulic conductivities for MW1, MW2, MW3, and MW4 determined using the Jacob–Ferris tidal methods and those determined by the Hvorslev slug test analysis method were not significantly different (Welch two sample t test $p=0.99$).

Water level response to tidal fluctuations

A tidally forced pattern in well water levels is primarily observed in wells MW2 and MW3 with a weaker signal in MW1 and MW4 (Figs. 2, 3). Throughout the study period, the relatively weak tidal signal in MW4 appears to wax (Fig. 3c) and wane (Fig. 3b). Signal processing analysis indicates that the fluctuations in water levels in these wells appear to lag tidal fluctuations by approximately 360 min (MW1 and MW4), 270 min (MW2), and 233 min (MW3). Unsurprisingly, the lag between fluctuations in water levels and tidal fluctuations increases with increasing distance from the Delaware River for the three wells along the perpendicular transect (Fig. 3). However, although MW1 and MW4 have similar lag times, MW1 is over twice as far from the Delaware River as MW4 is (480 versus 210 m) (Table 1).

Furthermore, the effect of tidal influence (i.e., the amplitude) in the wells along the perpendicular transect decreases as the distance to the Delaware River increases (Fig. 4). However, amongst all the wells that display a tidal influence (i.e., MW1, MW2, MW3, and MW4), the relationship between amplitude variations of M2 (the lunar semi-diurnal constituent) and the distance of the well from the shoreline (Fig. 4) appears to be more strongly influenced by the distance of the well from a historic sewer main. For example, the amplitude in MW4, located relatively more distant (57.8 m) from a sewer main (Table 1), is weak in comparison to the amplitudes of the other tidally influenced wells (i.e., MW1, MW2, and MW3). In MW1, MW2, and MW3, which are much closer to a sewer main (7.30 m) (Table 1), the M2 amplitude is relatively stronger, and decays roughly linearly with distance from the shoreline. Although MW5 and MW7 are installed at similar distances from the Delaware River (Fig. 1, Table 1), no tidal signal is present in these groundwater records (Figs. 2, 3). Moreover, although MW7 taps an aquifer with relatively conductive sediments, and water levels in this well are relatively consistent with Delaware River water levels (Fig. 3), no tidal signal is observed (Fig. 2).

Discussion

Nineteenth century sewer infrastructure influences tidal signal propagation and storm response

The tidal signal observed in wells MW1, MW2, MW3, and MW4 suggests there is heterogeneity within subsurface groundwater flow regimes in the US I-95 study area that most likely reflect the presence of 19th century combined sewer mains. Specifically, the waters in MW1, MW2, MW3, and periodically MW4 appear to experience a more direct exchange with Delaware River waters, whereas the other monitoring wells (i.e., MW5 and MW7) do not display any tidal signature or storm response, despite water levels in MW7 appearing relatively similar to those of the Delaware River (Fig. 3). Furthermore, while conceptually, amplitudes of tidally induced groundwater fluctuations should display an exponential decrease with decreasing distance from the shoreline (Mao et al. 2006), relationships between amplitudes and borehole distance from the shoreline in MW1, MW2, MW3, and MW4, are generally more variable (Fig. 4). These discrepancies could result from several processes, including preferential flow paths due to bedrock fractures, the topography of the pre-European settlement landscape, or legacy impacts from urbanization.

Analysis of early twentieth century sewer maps confirms that a combined sewer main is located in the immediate vicinity of (i.e., less than 5 m from) wells MW1, MW2, and MW3. Specifically, digitized maps of the main sewerage system of Philadelphia in 1902 place the Shackamaxon Relief Sewer directly next to the MW1, MW2, and MW3 transect and within 40 m of MW4 (Philadelphia Department of Public Works Bureau of Surveys 1902) (Fig. 5). Although MW4 is further from a sewer main, it is also closer to the Delaware River. The presumably less direct connection with sewer fill materials may therefore explain the weak tidal response in MW4 water levels (Figs. 2, 3b). Similarly, while slug tests suggest sediments near MW7 have a hydraulic conductivity relatively similar to those near MW1 and MW3, MW7 is nearly 0.5 km from the nearest sewer main (Table 1), thus limiting hydrologic connectivity with Delaware River tidal fluctuations. In summary, it is possible that the sewer bed, and the fill materials used to backfill it could serve as a conduit which would facilitate a relatively direct exchange of tidal fluctuations.

Implications for inundation from global sea level rise

Sea level rise driven by global climate change will likely interact with historic sewer infrastructure, posing unique

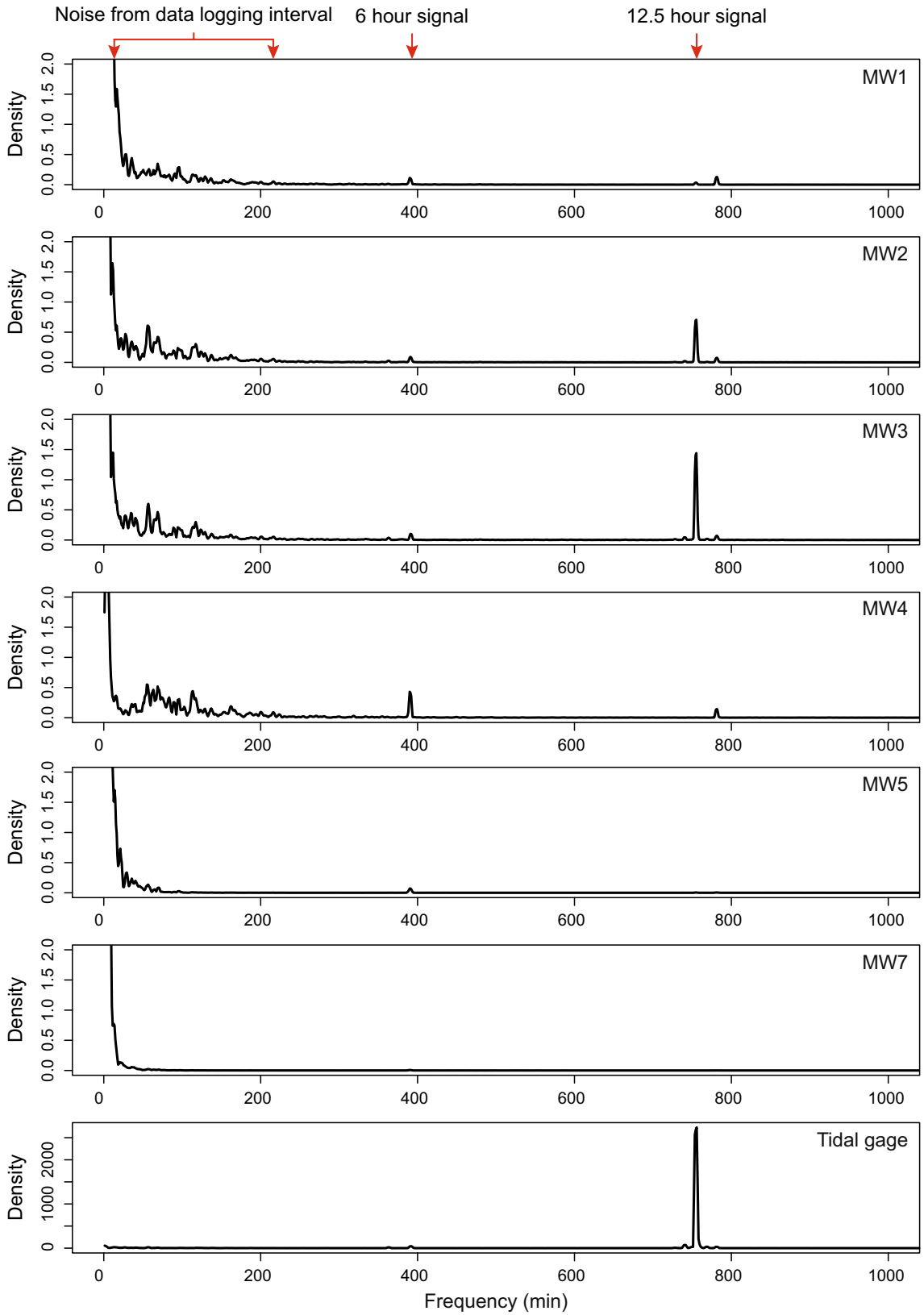

Fig. 2 Periodograms of harmonic frequencies for the tidal signal in wells MW1, MW2, MW3, MW4, MW5, MW7, and the Delaware River (NOAA Center for Operational Oceanographic Products and Services 2017)

challenges for coastal cities. In particular, inundation by groundwaters is predicted to affect coastal areas prior to inundation by sea water (Rotzoll and Fletcher 2012). As the water table rises along with rises in sea level (Bjerklie et al. 2012), groundwater will likely be forced along the conduits created by relatively high permeability fill materials (e.g., slag, coal ash) commonly used in the construction of historic urban sewer systems (Chirico and Epstein 2000). A similar mechanism has been observed in studies examining patterns of salt water intrusion in coastal aquifers (e.g., Goebel et al. 2017), where salt water intrusion has been observed to follow paleochannels in aquifer sediments. Such a disparate pattern of groundwater flow will likely create areas of mounded groundwater, potentially damaging infrastructure or the foundations or basements of nearby structures (Bjerklie et al. 2012).

Rises in local water tables, coupled with the age of sewer systems in coastal US cities, will likely also promote the infiltration of groundwater into sewer infrastructure (e.g., Bjerklie et al. 2012). Sewer age significantly affects the rate of sewer deterioration (Ana et al. 2008), and unsurprisingly, a recent survey by the US Environmental Protection Agency has highlighted 51.2 billion US dollars are needed to rehabilitate conveyance infrastructure in the US (United States Environmental Protection Agency 2016). Thus, these aging sewers are likely to have cracks that would facilitate an increased amount of infiltration of groundwater if water tables were to rise.

Increases of groundwater infiltration rates into sewer systems, coupled with global climate shifts will likely exacerbate flooding risk in coastal US cities. Presumably, increased rates of groundwater infiltration into sewer lines will increase sewer baseflow, which in turn will decrease the capacity of sewer lines (Broadhead et al. 2013). Therefore, decreases in sewer capacity will likely increase rates of flooding in low-lying urban areas served by combined sewer systems. Recent work by Semadeni-Davies et al. (2007) suggests that predicted rates of urbanization coupled with an increased occurrence of extreme precipitation events from global climate change will worsen flooding associated due to overtaxed combined sewerage systems in Sweden. Similarly, the United Kingdom considers flooding from overloaded sewer systems to be a serious issue facing the country (Parliamentary Office of Science and Technology 2007). However, neither of these studies consider how increased rates of urbanization, increased amounts of precipitation from global climate change, and increased rates of groundwater infiltration driven by sea level rise, will interact to affect rates of urban flooding due to overloaded sewer systems.

Many other coastal US cities, in addition to Philadelphia, have aging sewer infrastructure, and thus increased rates of groundwater infiltration into combined sewer systems pose a significant flooding risk to a sizable population. In 1905 nearly 9200 km of the sewer lines in coastal US cities consisted of combined sewers (United States Bureau of the Census 1907), which are particularly prone

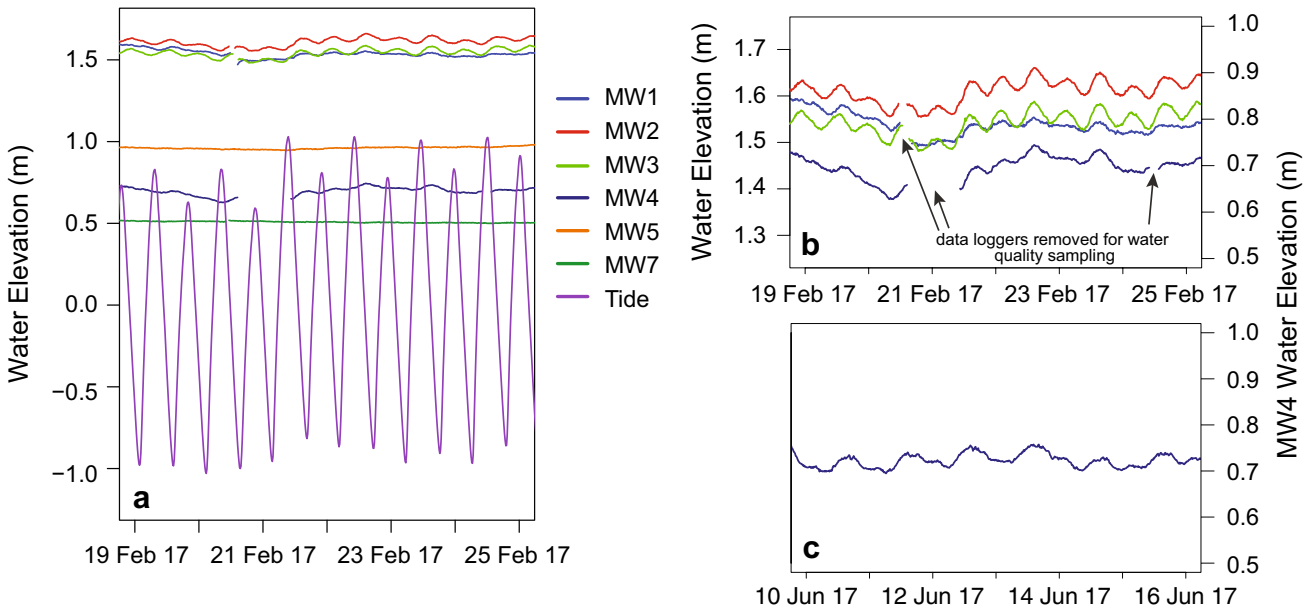

Fig. 3 Tidal fluctuations of the Delaware River (purple) (NOAA Center for Operational Oceanographic Products and Services 2017), water level elevations in wells MW1 (blue), MW 2 (red), MW3 (green), MW4 (dark blue), MW5 (orange), and MW7 (dark green), and panels detailing the tidal signals in MW1, MW2, MW3, and the weak tidal signature in MW4 (**a**), and a period where a relatively stronger tidal signature is observed in MW4 (**c**)

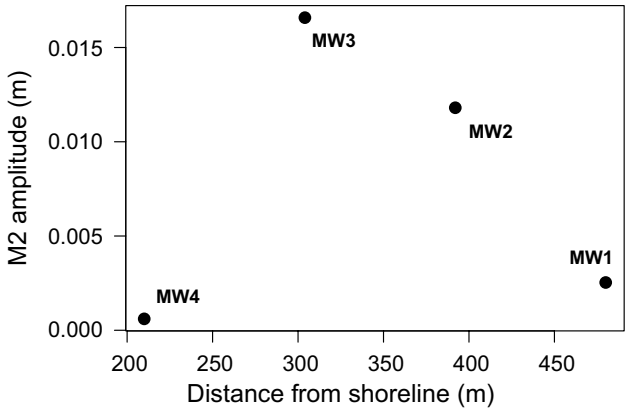

Fig. 4 Amplitude variations of M2 from fast-fourier transform analysis along monitoring wells perpendicular to US I-95

to flooding (Shuster et al. 2014). Currently these coastal cities have a combined population of nearly 26,400,000 (United States Census Bureau Population Division 2017). If only a fraction of these sewers was located in areas experiencing a raised water table due to global sea level rise, a relatively large population would be affected. Therefore, future research efforts should consider the interactions between shifts in precipitation, networks of historical sewerage infrastructure, and alterations of groundwater flow regimes to adequately constrain potential inundation risks to these coastal communities.

Conclusions

The response of water levels in monitoring wells to precipitation events, and tidal fluctuations in the study area displays the influence of a nearby early twentieth century combined sewer main on subsurface hydrological regimes. Specifically, water levels in the wells (MW1, MW2, MW3, and MW4) nearest to sewer mains are the most responsive to tidal fluctuations of the nearby Delaware River, despite the other monitoring wells being located at similar distances from the river. Moreover, slug tests demonstrate the hydrologic conductivities of aquifer sediments in the monitoring wells closest to a sewer main (i.e., within 5 m) (MW1, MW2, and MW3) are generally higher than the hydrologic conductivities of aquifer sediments in the other monitoring wells. Thus, the sewer bed, and the fill materials used to backfill likely serve as a conduit, facilitating a relatively direct exchange of tidal fluctuations of Delaware River waters.

Although interactions between tidally influenced groundwater fluctuations and historic sewer infrastructure are relatively under-characterized in the current literature, it is doubtful that these observations are unique to the study area. In particular, the extent and age of combined sewer systems in coastal US cities poses a significant risk of inundation due to rises in groundwater levels. Moreover, altered groundwater flow dynamics caused by sea level rise, coupled with climatic shifts will likely stress aging sewer infrastructure, leading to increased discharge of combined sewer overflow systems, or flooding associated with overloaded sewerage mains.

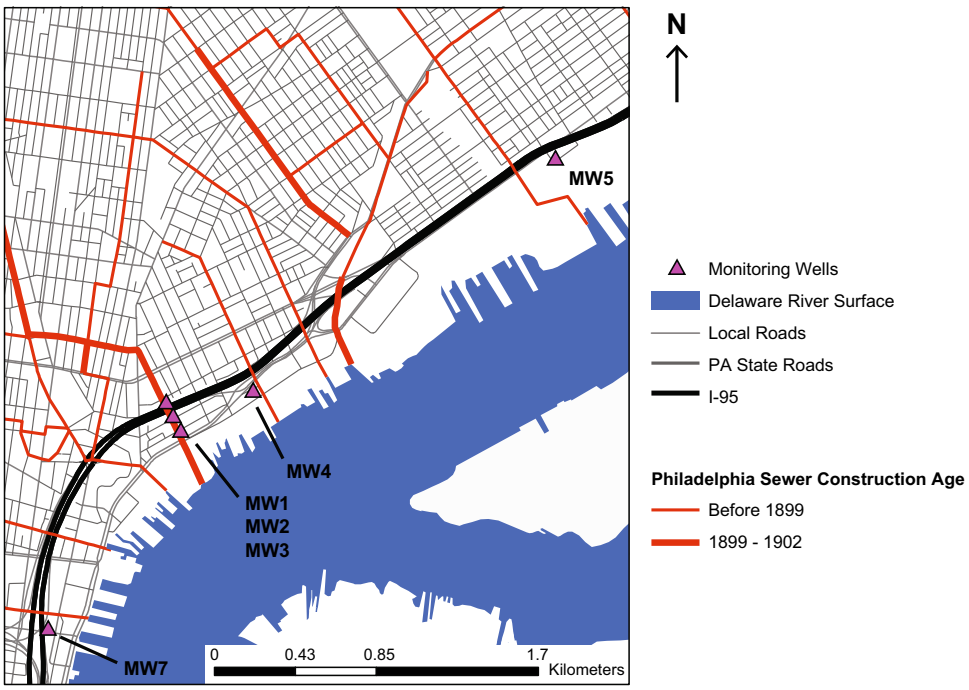

Fig. 5 The main sewerage system of Philadelphia in the study area in as of 1902 (Philadelphia Department of Public Works Bureau of Surveys 1902)

Acknowledgements The authors wish to thank Tyler Wong with assistance during well tests, and Juan Lezama with assistance during the spectral analysis. This work was funded by the Pennsylvania Department of Transportation under TEM WO 006 and a subcontract through AECOM.

References

Ana E, Bauwens W, Pessemier M, et al (2008) Investigating the effects of specific sewer attributes on sewer ageing a Belgian case study. In: 11th International Conference on Urban Drainage. Edinburgh, Scotland, UK, pp 1–10

Berg TM, Edmunds WE, Geyer AR, Glover AD, Hoskins DM, MacLachlan DB, Root SI, Sevon WD, Socolow AA (1980) Geologic map of Pennsylvania (2nd edition): Pennsylvania Geological Survey, 4th series, Map 1, 3 sheets, scale 1:250,000

Bhaskar AS, Welty C (2012) Water balances along an urban-to-rural gradient of metropolitan baltimore, 2001–2009. Environ Eng Geosci 18:37–50. https://doi.org/10.2113/gseegeosci.18.1.37

Bjerklie DM, Mullaney JR, Stone JR et al (2012) Preliminary Investigation of the effects of sea-level rise on groundwater levels in New Haven, Connecticut. US Geol Surv Open File Rep 2012:1–46

Broadhead AT, Horn R, Lerner DN (2013) Captured streams and springs in combined sewers: a review of the evidence, consequences and opportunities. Water Res 47:4752–4766. https://doi.org/10.1016/j.watres.2013.05.020

Broadhead AT, Horn R, Lerner DN (2015) Finding lost streams and springs captured in combined sewers: a multiple lines of evidence approach. Water Environ J 29:288–297. https://doi.org/10.1111/wej.12104

Bromley GW, Bromley WS (1895) Atlas of the city of Philadelphia, 1895. G.W. Bromley and Co., Philadelphia

Bromley GW, Bromley WS (1910) Atlas of the city of Philadelphia, 1910. G.W. Bromley and Co., Philadelphia

Chirico PG, Epstein JB (2000) Geographic information system analysis of topographic change in Philadelphia, Pennsylvania, during the last century. US Geol Surv Open-File Rep 2000:1–13

Delaware River Basin Commission (2019) Salt line location. https://www.state.nj.us/drbc/hydrological/river/salt-line.html. Accessed 18 March 2019

Divers MT, Elliott EM, Bain DJ (2013) Constraining nitrogen inputs to urban streams from leaking sewers using inverse modeling: implications for dissolved inorganic nitrogen (DIN) retention in urban environments. Environ Sci Technol 47:1816–1823. https://doi.org/10.1021/es304331m

Ellis JB, Revitt DM, Blackwood DJ, Gilmour DJ (2004) Leaky sewers: assessing the hydrology and impact of exfiltration in urban sewers. In: Webb B, Acreman M, Maksimovic C et al (eds) hydrology: science and practices for the 21st century. British Hydrological Society, Imperial College, London, pp 266–271

Ferris JG (1951) Cyclic fluctuations of water level as a basis for determining aquifer transmissibility. In: International Union of Geodesy and Geophysiscs, Association of Scientific Hydrology Assembly, pp 148–155

Fetter CW (2001) Applied hydrogeology, 4th edn. Prentice Hall, Upper Saddle River

Goebel M, Pidlisecky A, Knight R (2017) Resistivity imaging reveals complex pattern of saltwater intrusion along Monterey coast. J Hydrol 551:746–755. https://doi.org/10.1016/j.jhydrol.2017.02.037

Hibbs BJ, Sharp JM (2012) Hydrogeological impacts of urbanization. Environ Eng Geosci 18:3–24

Hopkins KG, Bain DJ, Copeland EM (2013) Reconstruction of a century of landscape modification and hydrologic change in a small urban watershed in Pittsburgh, PA. Landsc Ecol 29:413–424. https://doi.org/10.1007/s10980-013-9972-z

Jacob CE (1950) Flow of groundwater. In: Rouse H (ed) Engineering hydraulics. Wiley, New York, pp 321–386

Kim Y-Y, Lee K-K, Sung IH (2001) Urbanization and the groundwater budget, metropolitan Seoul area, Korea. Hydrogeol J 9:401–412. https://doi.org/10.1007/s100400100139

Lerner DN (1986) Leaking pipes recharge ground water. Groundwater 24:654–662. https://doi.org/10.1111/j.1745-6584.1986.tb03714.x

Machusick M, Welker A, Traver R (2011) Groundwater mounding at a storm-water infiltration BMP. J Irrig Drain Eng 137:154–160. https://doi.org/10.1061/(ASCE)IR.1943-4774.0000184

Mao X, Enot P, Barry DA et al (2006) Tidal influence on behaviour of a coastal aquifer adjacent to a low-relief estuary. J Hydrol 327:110–127. https://doi.org/10.1016/j.jhydrol.2005.11.030

Miles CE, Whitfield TG et al (2001) Bedrock geology of Pennsylvania: Pennsylvania Geological Survey, 4th series, dataset, scale 1:250,000. http://www.dcnr.state.pa.us/topogeo/publications/pgspub/map/map1/index.htm. Accessed 17 May 2017

NOAA Center for Operational Oceanographic Products and Services (2017) Observed Water Levels. https://tidesandcurrents.noaa.gov/waterlevels.html?id=8545240. Accessed 13 Mar 2017

Parliamentary Office of Science and Technology (2007) Urban flooding. POST Note 289:1–4

Paulachok GN (1991) Geohydrology and ground-water resources of Philadelphia. U.S. Geological Survey Water Supply Paper 2346

Pennsylvania Bureau of Topographic and Geologic Survey Deparment of Conservation and Natural Resources (1995) Physiographic Provinces 1:100,000. http://www.pasda.psu.edu. Accessed 17 May 2017

Pennsylvania Department of Transportation Bureau of Planning and Research Geographic Information Division (2017) PennDOT—pennsylvania stateroads. http://www.pasda.psu.edu. Accessed 17 May 2017

Philadelphia Department of Public Works Bureau of Surveys (1902) Main sewerage systems of the city of Philadelphia 1902. Dunlap Printing Co., Philadelphia

Philadelphia Water Department (2014) 2014 drinking water quality report. Philadelphia Water Department, Philadelphia, pp 1–25

Philadelphia Water Department (2017) Combined sewer area. http://www.phillywatersheds.org/what_were_doing/maps/kml. Accessed 15 May 2017

R Core Team (2016) R: A language and environment for statistical computing. R Foundation for Statistical Computing. Vienna, Austria. https://www.Rproject.org/

Rotzoll K, Fletcher CH (2012) Assessment of groundwater inundation as a consequence of sea-level rise. Nat Clim Chang 3:477–481. https://doi.org/10.1038/nclimate1725

Semadeni-Davies A, Hernebring C, Svensson G, Gustafsson L-G (2007) The impacts of climate change and urbanisation on drainage in Helsingborg, Sweden: combined sewer system. J Hydrol 350:100–113. https://doi.org/10.1016/j.jhydrol.2007.05.028

Seto KC, Fragkias M, Güneralp B, Reilly MK (2011) A meta-analysis of global urban land expansion. PLoS One 6:e23777. https://doi.org/10.1371/journal.pone.0023777

Sharp JM (2010) The impacts of urbanization on groundwater systems and recharge. Aqua Mundi 1:51–56. https://doi.org/10.4409/Am-004-10-0008

Shuster WD, Dadio S, Drohan P et al (2014) Residential demolition and its impact on vacant lot hydrology: implications for the management of stormwater and sewer system overflows. Landsc Urban Plan 125:48–56. https://doi.org/10.1016/j.landurbplan.2014.02.003

United Nations (2014) World Urbanization Prospects: The 2014 Revision, Highlights. Department of Economic and Social Affairs. Population Division, United Nations

United States Bureau of the Census (1907) Special Reports: statistics of cities having a population of over 30,000: 1905. Government Printing Office, Washington, DC

United States Bureau of the Census (2010) Census of the United States. Government Printing Office, Washington, DC

United States Census Bureau (2016) Cartographic boundary shapefiles—urban areas. https://www.census.gov/geo/maps-data/data/cbf/cbf_ua.html. Accessed 1 Jun 2017

United States Census Bureau Population Division (2017) Annual estimates of the resident population: April 1, 2010 to July 1, 2016. https://factfinder.census.gov/faces/nav/jsf/pages/index.xhtml. Accessed 16 Jun 2017

United States Environmental Protection Agency (2016) Report to Congress: Clean Watersheds Needs Survey 2012. Report EPA-830-R-15005

United States Geological Survey (2017) USGS water data for USA. In: Natl. Water Inf. Syst. https://waterdata.usgs.gov/nwis. Accessed 16 Jun 2017